Binding of Organic Anions by Synthetic Supramolecular Metallopores with Internal Mg^{2+} – Aspartate Complexes

Gopal Das,[a] Hisanari Onouchi,[b] Eiji Yashima,[b] Naomi Sakai,[a] and Stefan Matile*[a]

We report that cation-selective transmembrane pores formed by synthetic p*-octiphenyl* β *barrels with internal aspartate residues can be transformed into anion-permeable metallopores with internal* Mg^{2+} *– aspartate complexes. These metallopores are shown to be useful for fluorimetric sensing of a broad variety of organic anions of biological relevance such as phytate, heparin, thiamine phosphates, and adenosine triphosphate. The negligible flippase activity measurable for* Mg^{2+}*-free pores indicates that transmembrane* p*-octiphenyl* β *barrels do not disturb the lipid bilayer suprastructure, in other words, they form barrel – stave rather than toroidal pores.*

KEYWORDS:

bioorganic chemistry · fluorescence · lipid bilayers · molecular recognition · oligomers

Introduction

Straightforward synthetic access to transmembrane, large, and stable ion channels and pores[1–6] with variable internal active sites is required to exploit their confined interior in bioorganic chemistry and beyond. Controlled expansion of de novo α-helix bundles[3] into stable α barrels with well-defined architecture and variable internal functionality[7] remains difficult in bilayer membranes because little is known about how to avoid the formation of short-lived toroidal pores.[8] Roeske's elegant internal functionalization of stacked peptide macrocycles may become applicable to large interiors in the future.[4] The only practical synthetic route to multifunctional pores available today is self-assembly of *p*-octiphenyl "staves" with lateral peptide strands into rigid-rod[9] β barrels[10] such as pore **1** (Figure 1).[5, 6] The chemical nature of both the outer and inner surface of *p*-octiphenyl β barrels can be designed in a rational manner based on the $(i+2)$ repeat in the peptide β-sheet conformation. In pore **1**, for example, the sequence LDLDL was designed to result in external leucine residues for hydrophobic contact with the core of a lipid bilayer membrane and internal aspartate residues to create functionality along the central aqueous channel.[6]

Suprastructure determination of *p*-octiphenyl β barrels by conventional methods, which require micromolar or higher concentrations, is hampered by fibrillogenesis in solution[5d] and reorganization in bilayer membranes.[5h, 11a] At the nanomolar concentrations relevant for function, on the other hand, *p*-octiphenyl β barrels are among the best characterized class of synthetic ion channels and pores known today,[1–6] on both a functional and structural level. The following facts are known:

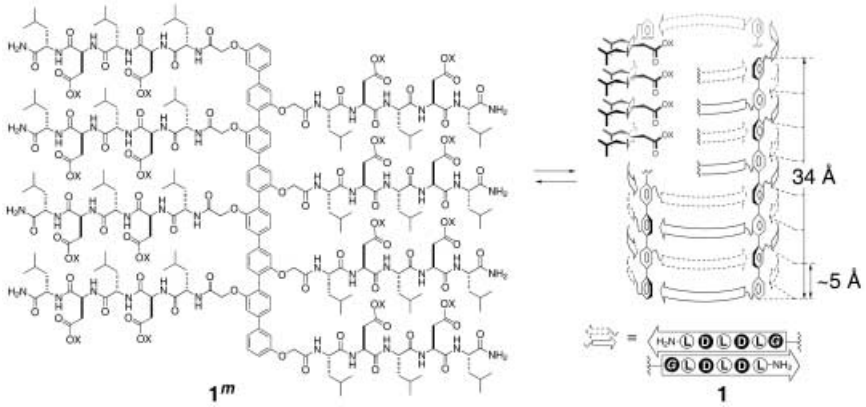

Figure 1. *Self-assembly of* p*-octiphenyl* β *barrels* ***1*** *from monomeric rods* $\mathbf{1^m}$*. Tetramer* ***1*** *is given as a schematic cutaway suprastructure with vertical distances estimated from molecular models,[12c] an axial M,P,M,P,M,P,M conformation implied by the all-*S α *amino acid configuration, and* β *strands depicted as arrows pointing towards the C terminus. External* α*-hydroxy and* α *amino acid residues (one-letter abbreviations are used; G: OCH*$_2$*CO) are black on white and internal residues are white on black. X = H, M; M = metal ion: 0.5 Mg, 1.0 Na, etc. depending on conditions.*

[a] *Prof. S. Matile, Dr. G. Das, Dr. N. Sakai*
Department of Organic Chemistry
University of Geneva
1211 Geneva 4 (Switzerland)
Fax: (+41) 22-328-7396
E-mail: stefan.matile@chiorg.unige.ch.

[b] *Dr. H. Onouchi, Prof. E. Yashima*
Department of Molecular Design and Engineering
Graduate School of Engineering, Nagoya University
Chikusa-ku, Nagoya 464-8603 (Japan)

  1439-4227/02/03/11 $ 20.00+.50/0

Transmembrane *p*-octiphenyl[2o, 5e, 5h, 11, 12] (and *p*-septiphenyl[12] but not *p*-sexiphenyl[11]) orientation has been confirmed in several instances by fluorescence depth quenching. The number of monomers per barrel has been determined for several examples from the nonlinear concentration dependence of the activity in bilayer membranes[5a, 5e, 6] and by size exclusion chromatography and circular dichroism (CD) Job plots in water.[13] Internal barrel diameters have been measured by single channel conductances,[5c, 5e, 5h, 5j] and dye leakage experiments.[5c, 5e, 5f, 5i, 5j, 6] Barrel stabilities have been determined from single channel lifetimes[5c, 5e, 5h, 5j] and correlated with barrel length[13a] by CD denaturation in solution.[5b, 13] AFM images of barrels have been recorded.[5d] The ultimate proof of principle for synthetic ion channels and pores, that is, meaningful and substantial blockage,[14] has been reported for *p*-oligophenyl channels and pores with internal lysines (with olignucleotide duplexes),[5f] histidines (with pyrene-1,3,6-sulfonates),[5c, 5j] aspartates (with $(Mg^{2+}{}_n \cdot ANTS_{n'})_{n''}$ complexes; ANTS = 8-aminonaphthalene-1,3,6-trisulfonate),[6] and arene arrays (with tetraethyl ammonium cations).[12a]

The objective of this study was to explore the potential of multifunctional pores formed by *p*-octiphenyl β barrel **1** for noninvasive fluorescence sensing applications. The synthesis of $1^3,2^3,3^2,4^3,5^2,6^3,7^2,8^3$-octakis(Gla-Leu-Asp-Leu-Asp-Leu-NH_2)-*p*-octiphenyl (**1*m***) and self-assembly into tetrameric pore **1** have been described previously.[6] Consistent with the "internal-charge-repulsion" model[5i] for the synthesis of transmembrane, large, and functionalized space, pore **1** exhibits nanomolar activity at $5 < pH < 7$.[6] Previous results further demonstrate the important possibility to inactivate pore **1** with internal $(Mg^{2+}{}_n \cdot ANTS_{n'})_{n''}$ complexes.[6] Both pH gating of, and $(Mg^{2+}{}_n \cdot ANTS_{n'})_{n''}$ binding within pore **1** have been supported with structural studies by CD spectroscopy.[6]

Here, we report that cation-selective "apopore" **1** can be progressively "filled", first with Mg^{2+} ions to give anion-permeable metallopore $\mathbf{1} \supset Mg^{2+}{}_n$, and then with various organic anions of biological relevance to form inactive inclusion complexes $\mathbf{1} \supset (Mg^{2+}{}_n \cdot guest_{n'})_{n''}$ (Figure 2). The cation selectivity of apopore **1** was further exploited to confirm that *p*-octiphenyl β barrels do not disturb the lipid bilayer structure, that is, that they form true barrel – stave structures and not, like many de novo α barrels,[8] toroidal pores.

Results and Discussion

Ion selectivity and cation binding

The activity of apopore **1** has been assessed previously by using the ANTS/DPX assay (DPX = *p*-xylenebis(pyridinium)bromide).[6] In this assay, efflux of either anionic ANTS or cationic DPX from spherical bilayers (here small unilamellar vesicles (SUVs) composed of fresh egg yolk phosphatidylcholine (EYPC)) is detected by an increase in ANTS emission intensity.[15] The ANTS/DPX assay is ideal for determination of the pH profile of large pores because ANTS emission is pH independent and ANTS/DPX efflux does not depend strongly on changes in ion selectivity with pH.[5i, 6, 15, 3d, 3i, 3j] However, the ANTS/DPX assay turned out to be incompatible with the characterization of metallopore $\mathbf{1} \supset Mg^{2+}{}_n$ (Figure 2) because the directly formed complex $\mathbf{1} \supset (Mg^{2+}{}_n \cdot ANTS_{n'})_{n''}$ is transport inactive (Figure 3, ○).[6]

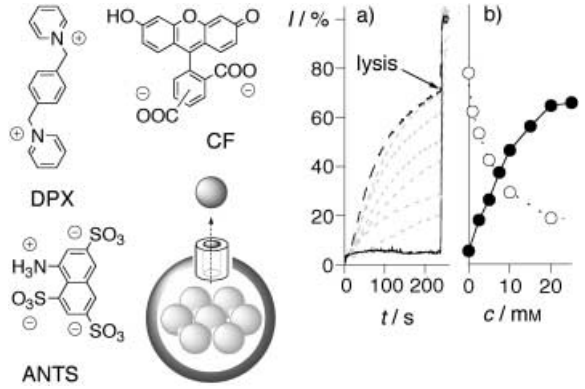

Figure 3. *Schematic representation of the assays and dose response CF (● and (a)) and ANTS/DPX (○, data from ref. [6]) curves for $Mg(OAc)_2$. a) Changes in CF emission at pH 6.5 as a function of time after addition of pore **1** (50 nM), $Mg(OAc)_2$ (from 0 (solid line) to 25 mM (dashed lines)) to and at lysis (50 μL 1.2% aq Triton X-100) of EYPC-SUVs ⊃ CF (250 μM); b) I^{200} values (%) for (a) and ANTS/DPX studies (see the Experimental Section for details).*

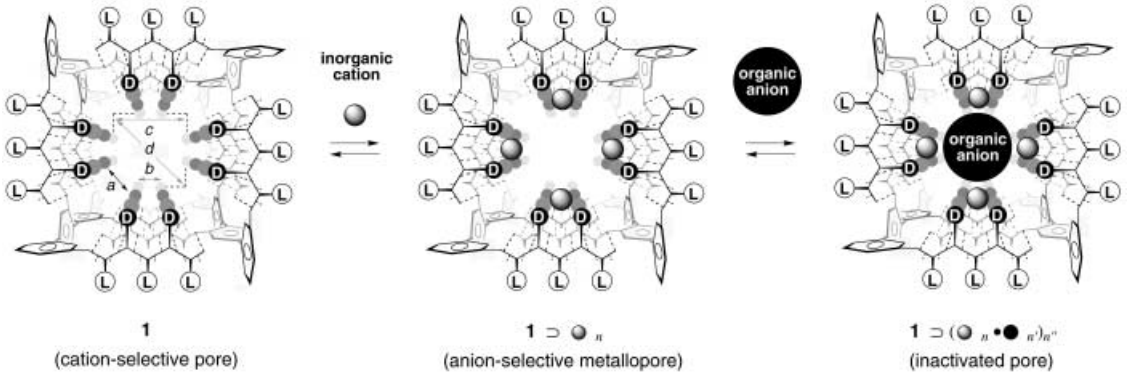

Figure 2. *Design of internal cation binding to apopore **1** and anion binding to metallopore $\mathbf{1} \supset Mg^{2+}{}_n$. Horizontal distances, estimated from molecular models: a ≈ 4, b ≈ 7, c ≈ 12, d ≈ 17 Å.[13c] β strands are indicated as solid (backbone) and dotted lines (hydrogen bonds) in the schematic axial views. Compare Figure 1 for structural details and vertical distances and Table 1 for details of the organic anions.*

The CF assay was thus selected for the study of anion binding by metallopore **1** ⊃ $Mg^{2+}{}_n$. This assay is based on spherical bilayers (here EYPC-SUVs) that are loaded with anionic 5(6)-carboxyfluorescein (CF) at self-quenching concentrations.[15, 2o, 5e, 5f, 11a] CF efflux through large enough pores is detected by an increase in CF emission intensity caused by dilution. In contrast to the ANTS/DPX assay, the CF assay is dependent on the ion selectivity of the pore and only applicable at pH values above the pK_a value of CF (6.3).

In contrast to results from the ANTS/DPX assay, addition of up to 50 nM rigid-rod β barrel **1** to EYPC-SUVs ⊃ CF did not cause detectable CF efflux at pH 6.5 (Figure 3a, solid line).[16] This deceptive inactivity suggested that pores **1**, which are active according to the ANTS/DPX assay, are either too small or too anionic to let the bulky anion CF pass through. Electrostatic rather than steric repulsion was indicated by the activation of CF efflux through cation-selective apopore **1** by addition of $Mg(OAc)_2$, that is, formation of an anion-permeable metallopore **1** ⊃ $Mg^{2+}{}_n$ (Figure 3a, dotted and dashed lines; Figure 3b, ●; dissociation constant, $K_D = 5.3$ mM). This interpretation is supported by the identification of a global barrel suprastructure in the presence and absence of $Mg(OAc)_2$ described previously[6] as well as all the results from flippase assays and anion binding to metallopore **1** ⊃ $Mg^{2+}{}_n$ described in the following text.

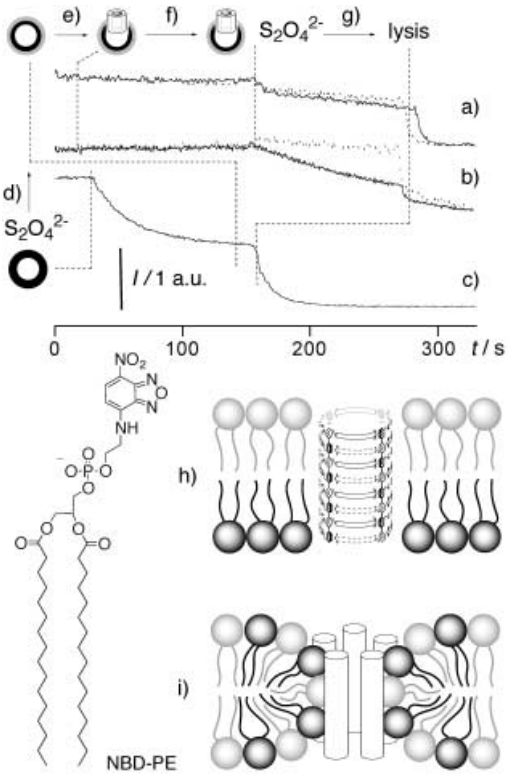

Figure 4. *Flippase assay in the absence (dotted line) and presence (solid line) of apopore **1** (12.5 nM) in nitrobenzofurazan-phosphatidylethanolamine (NBD-PE)/EYPC-SUVs (250 μM), (a) without and (b) with $Mg(OAc)_2$ (20 mM) at pH 6.4. c) Outer and inner leaflet reduction: (NBD-PE)/EYPC-SUVs (250 μM) with sodium dithionite (10 mM) without pore **1** and $Mg(OAc)_2$ for calibration and proof of unilamellarity. a, b) Change in NBD emission ($\lambda_{ex} = 463$ nm, $\lambda_{em} = 536$ nm) of (d) outer-leaflet-reduced (NBD-PE)/EYPC-SUVs (250 μM) during (e) addition of **1** (12.5 nM), (f) approximately 100 sec incubation, (g) addition of sodium dithionite (10 mM), and lysis (40 μL 10% aq Triton X-100) to reveal the (h) barrel – stave rather than (i) toroidal suprastructure of apopore **1** (a) and the anion permeability of the metallopore (b). 1 a.u. = 1 arbitrary unit, which corresponds to the relative change in NBD emission for one leaflet reduction.*

Flippase activity, ion selectivity, and cation binding

Experimental evidence for the first cation-selective pore formed by rigid-rod β barrels provided the opportunity to assess their flippase activity for the first time. The flippase assay is of central importance for the determination of active suprastructures because it distingushes between so-called barrel – stave pores (Figure 4h) and toroidal pores (Figure 4i).[8] Stable barrel – stave pores represent a popular suprastructural model that does not affect the rate of lipid flip-flop between the outer and inner leaflets of the bilayer. The more recent concept of short-lived toroidal pores is, however, attracting increasing scientific attention since experimental evidence for flippase activity of most (but not all) putative α barrels[7] formed by amphiphilic α helices in membranes has become available.[8]

The flippase activity of pore **1** was determined by following the procedure of Matsuzaki and coworkers, with minor modifications.[8a] This assay employs EYPC-SUVs that are labeled with 0.25 mol% NBD-PE. Quenching of the NBD fluorophore by a reductant (sodium dithionite) is observed by fluorescence kinetics in order to monitor the change in accessibility of NBD groups on the bilayer surface. After preparation of the vesicles, NBD groups on the outer surface of the vesicles were reduced to give the inner-leaflet-labeled vesicles (Figure 4d). These vesicles were then incubated with pore **1** in the presence (Figure 4b) and absence (Figure 4a) of Mg^{2+} ions to allow lipid flip-flop to take place (Figure 4f). If toroidal rather than barrel – stave pores form, NBD groups initially located on the inner surface should translocate to the outer surface (Figure 4i), and addition of reductant after incubation should reveal flip-flop (Figure 4g).

Comparison of inner leaflet accessibility with and without *p*-octiphenyl β barrel **1** revealed negligible flippase activity (Figure 4a). This finding thus demonstrated formation of barrel – stave (Figure 4h) rather than toroidal (Figure 4i) pores, a result expected from the overall high stability of single channels formed by *p*-octiphenyl β barrels.[5c, 5e, 5h, 5j] An increase in "activity" was observed in the presence of $Mg(OAc)_2$ (Figure 4b). $Mg(OAc)_2$ thus either induced flippase activity or a loss in cation selectivity by pore **1**, which allowed the dithionite to pass through the pore and reach the NBD fluorophore at the inner interface. The ion selectivities identified with the CF assay (cation transport by anionic pore **1** and anion transport by metallopore **1** ⊃ $Mg^{2+}{}_n$; Figure 3) demonstrated that a loss of cation selectivity occurs.

Anion binding

Binding of organic anions by metallopore **1** ⊃ $Mg^{2+}{}_n$ (Figure 2) was studied by using the CF assay described above (Figure 3). Changes in activity of metallopore **1** ⊃ $Mg^{2+}{}_n$ caused by increasing concentrations of vitamin B1, thiamine monophosphate, and thiamine pyrophosphate are depicted in Figure 5a – c. Hill plots

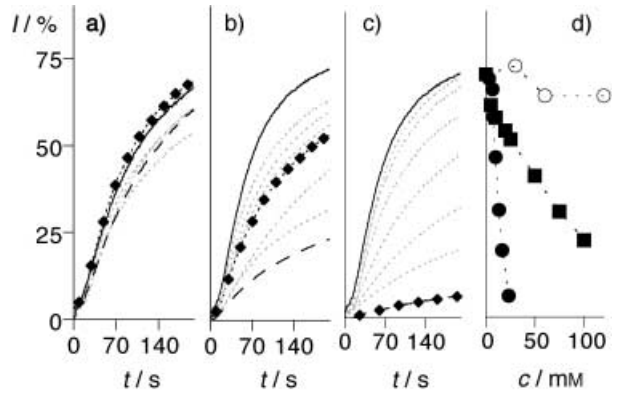

Figure 5. *Dose response CF curves for thiamine, thiamine phosphate, and thiamine pyrophosphate. (a – c) Changes in CF emission at pH 6.5 as a function of time after addition of pore* ***1*** *(50 nM), $Mg(OAc)_2$ (10 mM), and (a) thiamine (from 0 (solid line) to 30 (◆) and 240 mM (dashed line)), (b) thiamine phosphate (from 0 (solid line) to 30 (◆) and 100 mM (dashed line)), and (c) thiamine pyrophosphate (from 0 (solid line) to 23 mM (dashed line and ◆)) and before lysis (50 μL 1.2% aq Triton X-100) of EYPC-SUVs ⊃ CF (250 μM). (d) I^{200} values (%) for (a – c); ○ = thiamine, ■ = thiamine phosphate, ● = thiamine pyrophosphate (see the Experimental Section for details).*

of dose response curves (Figure 5 d) gave apparent dissociation constants for the thiamine (Table 1, entries 1 – 3) as well as the inorganic phosphate (entries 4 – 7), adenosine phosphate (entries 8 – 11), and glucose phosphate series (entries 12 – 14).[17] Organic anions reduced efflux rates rather than the final extent of CF release, therefore it was not possible to determine K_D values at thermodynamic equilibrium. The reported values thus represent an internally consistent data set that is conditional on the applied analytical procedure.

In general, neutral (entries 1 and 20) and phosphodiester guests (entry 8) exhibited poor capacity to block metallopore **1** ⊃ $Mg^{2+}{}_n$. Consistent with known K_D values for Mg^{2+} ion binding,[17b] phosphate monoesters (entry 2, 9, 12 – 16) were overall less potent than phosphoric anhydrides (entries 3, 5 – 7,[18] 10, 11). Frequent coincidence of low K_D values, low Hill coefficients *n* and high guest valence *N* (entries 7, 17, 18) supported multiple monomer binding on the one hand and multivalent oligomer and polymer binding on the other.

Topological matching may contribute to some exceptions from the trends described above. High K_D values were observed despite high *N* values for more bulky guests such as the environmentally relevant phytate[19] (entry 16) and heparin,[20] a sulfated polysaccharide of medicinal importance (entry 19). In contrast, the exceptionally low K_D values for rigid, planar PTS (entry 18), semi-rigid rods **2** (entry 17) and polyphosphate (entry 7), were in excellent agreement with preorganized, multivalent binding to the topologically complementary interior expected for metallopore **1** ⊃ $Mg^{2+}{}_n$ (Figure 1).[21, 18]

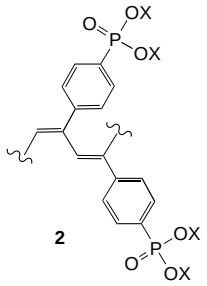

2

Structural studies by circular dichroism spectroscopy

CD spectroscopy has been used previously to correlate pH-gated pore formation with *p*-octiphenyl β-barrel suprastructure **1**. This tertiary structure is characterized by a typical, negative first CD Cotton effect at 305 nm that originates from L_a transitions of the chiral rigid-rod chromophore (Figure 6 b, solid line).[6, 13] CD

Table 1. *Anion binding characteristics of metallopore* ***1*** ⊃ $Mg^{2+}{}_n$.[a]

Entry	Guest	*N*[b]	Blockage [%][c]	*n*[d]	K_D [mM]
1	thiamine (vitamin B1)	0	0	-	> 240.0
2	thiamine phosphate	1	100	0.9	30.0
3	thiamine pyrophosphate	2	100	3.4	10.0
4	inorganic phosphate (P_i)	1	30	4.4	66.6
5	pyrophosphate (PP_i)	2	100	2.8	5.5
6	triphosphate (PPP_i)	3	100	2.3	2.2
7	polyphosphate	61	100	1.9	0.09[e]
8	cAMP[f]	1	0	-	> 80.0
9	AMP[f]	1	40	1.4	20.4
10	ADP[f]	2	100	1.5	6.3
11	ATP[f]	3	100	1.8	6.7
12	D-glucose 6-phosphate (G-6-P)	1	50	2.2	49.0
13	α-D-glucose 1-phosphate (G-1-P)	1	100	1.1	24.7
14	α-D-glucose 1,6-diphosphate (G-1,6-PP)	2	100	2.2	11.2
15	D-fructose 1,6-diphosphate	2	100	3.8	21.8
16	phytate (IP_6)	6	100	3.0	30.5
17	poly((4-phosphonophenyl)acetylene) **2**	620	100	1.0	0.008[f]
18	pyrene-1,3,6,8-tetrasulfonate (PTS)	4	100	1.8	0.7
19	heparin	36	100	1.4	11.6[f]
20	imidazole	0	0	-	> 300.0

[a] Data determined from Hill plots [Eq. (3)] of dose response curves for blockage of CF efflux from EYPC-SUVs ⊃ CF in the presence of metallopore **1** ⊃ $Mg^{2+}{}_n$, as exemplified in Figures 5 – 7; all reported values are internally consistent but conditional on this procedure. [b] *N* = Number of RPO_2XR'/RSO_3X groups per (macro)molecule as an approximate value for valence (X = H, M (M = metal ion: 0.5 Mg, 1 Na, etc.) depending on anion structure and conditions). [c] Maximum metallopore inactivation by organic anion guests observed in or extrapolated from dose response curves. [d] *n* = Hill coefficient [Eq. (3)]. [e] Calculated based on average molecular weight. [f] cAMP = cyclic adenosine monophosphate, ADP = adenosine diphosphate, ATP = adenosine triphosphate.

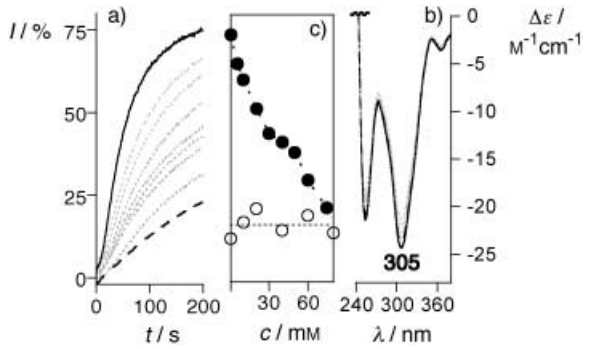

*Figure 6. Dose response CF and CD curves for α-D-glucose1-phosphate. a) Change in CF emission at pH 6.5 as a function of time after addition of pore **1** (50 nM), $Mg(OAc)_2$ (10 mM), and G-1-P (from 0 (solid line) to 75 mM (dashed line)) at and before lysis (50 μL 1.2% aq Triton X-100) of EYPC-SUVs ⊃ CF (250 μM). b) CD spectra of **1** (1.25 μM) at pH 6.5 in the presence of EYPC-SUVs (250 μM), $Mg(OAc)_2$ (10 mM), and G-1-P (from 0 (solid line) to 80 mM (dashed line)). Path length of CD cell = 1.0 cm. c) I^{200} values for (a) (●) and $\Delta\varepsilon^{305}$ values for (b) (○). See the Experimental Section for details.*

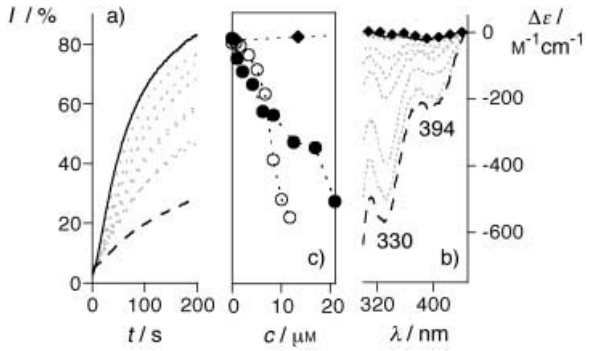

*Figure 7. Dose response CF and CD curves for poly((4-phosphonophenyl)acetylene) (**2**). a) Change in CF emission at pH 6.5 as a function of time after addition of pore **1** (50 nM), $Mg(OAc)_2$ (10 mM), and **2** (from 0 (solid line) to 13 μM (dashed line)) and before lysis (50 μL 1.2% aq Triton X-100) of EYPC-SUVs ⊃ CF (250 μM). b) CD spectra of **2** (from 0 (solid line) to 13 μM (dashed line and ◆)) at pH 6.5 in the presence of EYPC-SUVs (250 μM), $Mg(OAc)_2$ (20 mM), and **1** (1.25 μM; ◆: 0 mM). Path length of CD cell = 0.1 cm. c) I^{200} values for (a) (●) and $\Delta\varepsilon^{330}$ values for (b) (○ and ◆). See the Experimental Section for details.*

spectroscopy has further been used to confirm that the β-barrel suprastructure does not change with Mg^{2+} binding.[6]

α-D-glucose 1-phosphate (G-1-P) was selected as a nonchromophoric guest of metallopore **1** ⊃ $Mg^{2+}{}_n$ to elucidate changes in β-barrel suprastructure during guest binding. Almost complete inhibition of CF efflux through metallopore **1** ⊃ $Mg^{2+}{}_n$ indicated internal G-1-P binding with an apparent $K_D = 24.7$ mM (Figure 6a and Table 1, entry 13). In clear contrast to this result, the characteristic β-barrel CD spectrum of metallopore **1** ⊃ $Mg^{2+}{}_n$ (Figure 6b, solid line) did not change in the presence of up to 80 mM G-1-P (Figure 6b, dashed line). Although measured at different barrel concentrations (the CD spectra of *p*-octiphenyl β barrels are not detectable at the nanomolar concentrations relevant for transport activity), comparison of CF (●) and CD binding curves (○) indicated that changes of metallopore **1** ⊃ $Mg^{2+}{}_n$ suprastructure during formation of the inclusion complex **1** ⊃ $(Mg^{2+}{}_n \cdot \text{phosphate}_{n'})_{n''}$ are as unlikely as guest-induced barrel extraction into the media.[6, 5f]

Binding of poly((4-phosphonophenyl)acetylene) (**2**) to metallopore **1** ⊃ $Mg^{2+}{}_n$ (Figure 7a and Table 1, entry 17) was of particular interest because the *cis-transoidal* polyene chromophore forms one-handed helices upon binding to chiral cations.[22] This characteristic offered the opportunity to secure direct structural evidence for the formation of inclusion complexes **1** ⊃ $(Mg^{2+}{}_n \cdot \text{phosphate}_{n'})_{n''}$.

The presence of EYPC-SUVs and $Mg(OAc)_2$ did not change the CD silence of poly((4-phosphonophenyl)acetylene) (Figure 7b; compare solid line and ◆). Metallopore **1** ⊃ $Mg^{2+}{}_n$, however, induced the appearance of negative Cotton effects at 394 nm and 330 nm for polyene **2** (Figure 7b, compare solid and dashed lines). The magnitude and energy of the observed CD Cotton effects differed from previous results on binding of chiral cations to poly((4-phosphonophenyl)acetylene).[22a] The origin of these differences is not understood. Contributions from changes in the helical conformation or pitch of the polyene,[22b] increasing negative contributions from EYPC-SUV scattering with increasing energy,[23] and polyene/pore-induced vesicle aggregation can therefore not be excluded as this stage. The CD Cotton effects of the *p*-octiphenyl chromophore (Figure 6b) are much weaker than those of poly((4-phosphonophenyl)acetylene) and thus not detectable under the conditions required to measure the poly((4-phosphonophenyl)acetylene) effects (Figure 7b).

Comparison of CF (●) and CD binding curves (○) for polyene **2** revealed excellent agreement with regard to the K_D values ($K_D \approx 8$ μM; Figure 7). However, the CD binding curve exhibited clearly higher cooperativity ($n = 5.0$). Although attractive speculations on the origin of this difference in pore inactivation and polyene chirality can be readily formulated, it is clear that further studies will be needed to understand this effect.

Concluding Remarks

We report that highly active, doubly pH-gated pores formed by *p*-octiphenyl β barrels **1** do not disturb the structure of the surrounding lipid bilayer. This experimental evidence for the formation of barrel – stave rather than toroidal pores became available as a result of the cation selectivity of **1**, unprecedented for *p*-octiphenyl β barrels. The finding is an important addition to the suprastructural characterization of *p*-octiphenyl β-barrel pores under the conditions relevant for activity summarized in the introduction and is also important because it underscores the previously noted[5h, 5i] difference between *p*-octiphenyl β-barrel pores and transient toroidal pores formed by many de novo "α barrels".

We discovered that these cation-selective barrel – stave apopores **1** can be transformed into anion-permeable metallopores which, in turn, can serve as a sensor for a broad variety of organic anions in a clear-cut, reliable, and general manner. Studies on ways to exploit this remarkably clean and broad adaptability for practical sensing applications are ongoing.

From a methodological point of view, it is worthwhile to note how easily the superb, nanomolar activity of apopore **1** could be

overlooked in the CF assay. The same can be said for metallopore **1** ⊃ Mg^{2+}_n in the ANTS/DPX assay. Moreover, results from the flippase assay could be misintepreted as flippase activity of metallopore **1** ⊃ Mg^{2+}_n without the backup of results on ion selectivity from CF and ANTS/DPX assays. The overall lesson is not new but important: identification and characterization of synthetic ion channels and pores requires increasing caution with increasing selectivity of either pore or assay. The least selective and thus most suitable assay for initial screening remains, in our opinion and despite many disadvantages, the 8-hydroxypyrene-1,3,6-trisulfonate assay.[5, 15]

Experimental Section

General: As in the Supporting Information of ref. [2o)]. EYPC was from Avanti, CF and NBD-PE from Molecular Probes, buffers and guests listed in Table 1 except **2** were from Sigma and Fluka-Aldrich. "Triphosphate" refers to pentasodium tripolyphosphate (Sigma) and "polyphosphate" to sodium phosphate glass Type 65 (Sigma). The average molecular weight of a 61-mer determined by Sigma was used. Heparin was of an average molecular weight of 6000 (Sigma). Valence N (≈36) was approximated assuming an average molecular weight of 500 for heparin disaccharides with three RSO_3X groups.

Poly((4-phosphonophenyl)acetylene) (2): Polyene **2** was synthesized as in ref. [22a)]. An average molecular weight of 148 000 for the phosphodiethylester precursor of **2** was determined by size exclusion chromatography against poly(ethylene oxide) standards in dimethylformamide that contained LiCl (10 mM; $M_w/M_n = 1.9$). This result corresponds to an average molecular weight of 113 800 for polyphosphonate **2** and an average N value of 620. Aqueous stock solutions of **2** were prepared by mixing buffer A (2-[4-(2-hydroxyethyl)-1-piperazinyl]ethanesulfonic acid (HEPES; 10 mM), NaCl (107 mM); $n \times 1.0$ ml, pH 7.4) with NaOH ($n \times 0.3$ mL, 0.2 M) to give buffer B. Buffer B was degassed by freezing under vacuum and thawing under Ar (3 ×) to give buffer C. Then **2** ($n \times 16.1$ mg) was dissolved in buffer C ($n \times 1.7$ mL) to give stock solutions (83.4 μM per polymer; 52 mM phosphonate). The UV/Vis spectrum of **2** was as reported previously.[22a] Fresh stock solutions were calibrated by following the general procedure below, kept in the dark, and used within 24 h.

1^3,2^3,3^2,4^3,5^2,6^3,7^2,8^3-Octakis(Gla-Leu-Asp-Leu-Asp-Leu-NH_2)-*p*-octiphenyl 1^m: Rod 1^m was synthesized and purified as in ref. [6]. Stock solutions of 1^m were prepared in MeOH, and the *p*-octiphenyl concentration was confirmed by UV/Vis spectroscopy in water [ε (*p*-octiphenyl) = 28.6 $mM^{-1}\,cm^{-1}$ (320 nm)].[11a]

CF assay: This pH-sensitive dye-leakage assay[15] was performed by following the procedure used previously in the Geneva laboratory for diverse applications, without modification.[2o, 5e, f, 11a]

Vesicle preparation: EYPC-SUVs ⊃ CF stock solutions (EYPC (10 mM); inside: CF (50 mM), HEPES (10 mM), NaCl (10 mM), pH 7.4; outside: HEPES (10 mM), NaCl (107 mM), pH 7.1) were prepared as described previously (diameter: 68 ± 4 nm).[2o, 5e, f, 11a]

Cation binding: EYPC-SUVs ⊃ CF (50 μL) and buffer (1.95 mL; HEPES (10 mM), NaCl (107 mM), pH 6.5) were placed in a thermostated cell. Changes in relative fluorescence intensity (I_t, $\lambda_{em} = 510$ nm, $\lambda_{ex} =$ 495 nm, FluoroMax-2, Jobin Yvon-Spex) were recorded as a function of time during addition of $Mg(OAc)_2$ (0 mM: Figure 3, solid line; 2.5, 5.0, 7.5, 10.0, 15.0, 20.0, 25.0 mM: dashed lines; final concentrations indicated), **1** (50 nM) at time A [emission I at time A corresponds to I_0 in Eq. (1)], and Triton X-100 (50 μL, 1.2% aq) at time B [emission I at B + 50 s corresponds to I_∞ in Eq. (1)] to the gently stirred vesicle suspension. CF binding curves (Figure 3, ●) and Hill plots for Mg^{2+} binding were prepared by following the general procedure below.

Anion binding: EYPC-SUVs ⊃ CF (50 μL) and buffer (1.95 mL; HEPES (10 mM), NaCl (107 mM), pH 6.5) were placed in a thermostated cell. Changes in relative fluorescence intensity (I_t, $\lambda_{em} = 510$ nm, $\lambda_{ex} =$ 495 nm) were recorded as a function of time during addition of $Mg(OAc)_2$ (10 mM final concentration), guest (0 – 300 mM as appropriate; see Table 1 for guest structures and concentrations), barrel **1** (50 nM) at time A [emission I at time A corresponds to I_0 in Eq. (1)], and Triton X-100 (50 μL, 1.2% aq) at time B [emission I at B + 50 s corresponds to I_∞ in Eq. (1)] to the gently stirred vesicle suspension. CF binding curves and Hill plots for guest binding were prepared following the general procedure below, illustrated in Figures 5 – 7, and summarized in Table 1. Caution: Preparation of guest stock solutions as described in the next paragraph (Figure 8) is a prerequisite for valid anion binding experiments.

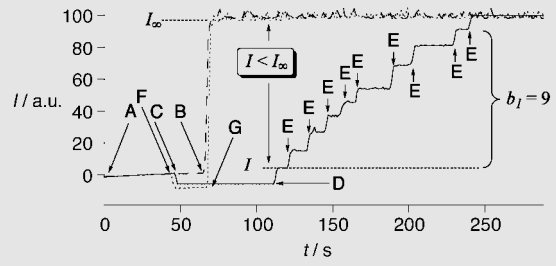

Figure 8. *Representative reference (dashed line), calibration (solid line), and control (dotted line) curves for the preparation of guest stock solutions as described in the text. a.u. = arbitrary units [not normalized with Eq. (1)].*

Preparation of stock solutions for anion binding: Representative reference (dashed line), calibration (solid line), and control (dotted line) curves are shown in Figure 8 to clarify the following procedure, which takes advantage of the pH sensitivity of CF ($pK_a = 6.3$).[15] Reference curve: EYPC-SUVs ⊃ CF (50 μL) and buffer (1.95 mL; HEPES (10 mM), NaCl (107 mM), pH 6.5) were placed in a thermostated cell. Changes in fluorescence intensity ($\lambda_{em} = 510$ nm, $\lambda_{ex} = 495$ nm) were measured as a function of time during addition of (A) $Mg(OAc)_2$ (10 mM final concentration) and (B) Triton X-100 (50 μL, 1.2% aq) to the gently stirred vesicle suspension to give I_0. Calibration curve: EYPC-SUVs ⊃ CF (50 μL) and buffer (1.95 mL; HEPES (10 mM), NaCl (107 mM), pH 6.5) were placed in a thermostated cell. Changes in fluorescence intensity ($\lambda_{em} = 510$ nm, $\lambda_{ex} = 495$ nm) were measured as a function of time during addition of (A) $Mg(OAc)_2$ (10 mM final concentration), (C) guest stock solution (a_1 μL, a_2 M) with a total volume of $n \times a_1$ μL (a_1/a_2 = highest volume of stock solution used/concentration envisioned for binding studies), and (D) Triton X-100 (50 μL, 1.2% aq) to the gently stirred vesicle suspension to give I. If $I < I_\infty$, NaOH ($b_1 \times 20$ μL, b_2 M; b_1 and b_2 are variables to be optimized) was added to reach $I \approx I_\infty$ during the same fluorescence time drive (E) as in the previous step. NaOH ($n \times b_1 \times 20$ μL, b_2 M) was then added to the guest stock solution (addition of a correspondingly smaller volume of more concentrated NaOH is preferable to minimize dilution). Control curve: EYPC-SUVs ⊃ CF (50 μL) and buffer (1.95 mL; HEPES (10 mM), NaCl (107 mM), pH 6.5) were placed in a thermostated cell. Changes in fluorescence intensity ($\lambda_{em} = 510$ nm, $\lambda_{ex} = 495$ nm) were measured as a function of time during addition of (A) $Mg(OAc)_2$ (10 mM final concentration), (F) calibrated guest stock solution (a_1 μL, a_2 M) and (G) Triton X-100 (50 μL 1.2% aq) to the gently stirred vesicle

suspension to give I'. Calibrated guest stock solutions with $I' \approx I_\infty$ are applicable for binding experiments.

Dose response CF curves and Hill plots: Flux curves were normalized to percent change in intensity I by using Equation (1), with I_t (time drive), I_0 (at addition of barrel), and I_∞ (after lysis) values as defined above.

$$I = \frac{(I_t - I_0)}{(I_\infty - I_0)} \times 100 \quad (1)$$

CF binding curves were prepared by plotting the leakage I (%) after a meaningful period of time (usually 200 – 250 s, i.e., I^{200} or I^{250} values) as a function of guest concentration. Controls indicated that plots of initial velocities or initial rate constants as a function of the parameter of interest gave the same results within experimental error. The fractional saturation Y was derived from Equation (2), where I_0^{200} is the I^{200} value from Eq. (1) without guest and I_∞^{200} is the I^{200} value at guest saturation.

$$Y = \frac{(I_0^{200} - I^{200})}{(I_0^{200} - I_\infty^{200})} \quad (2)$$

Hill plots for CF binding curves were calculated by using Equation (3),[6, 17a, 22a] where n is the Hill coefficient (indicative of multiple guest binding and/or positive cooperativity if $n > 1$), c_G is the guest concentration, and K_D is the apparent dissociation constant. The obtained K_D values are internally consistent but conditional upon this procedure.

$$\log(Y/(1-Y)) = n\log c_G - n\log K_D \quad (3)$$

Flippase assay: The flippase assay was performed by following Matsuzaki's procedure,[8a] with modifications.

Vesicle preparation: A solution of NBD-PE (0.16 mg, 0.16 μmol), EYPC (50 mg, 66 μmol) and sodium cholate (22.4 mg, 52 μmol) in $CHCl_3$ and MeOH (1 mL each) was dried under a stream of N_2 and then under a vacuum. Potassium phosphate buffer (1 mL; $K_mH_nPO_4$ (10 mM), KCl (100 mM), pH 6.4) was added to the resulting thin film and the mixed micelle dispersion was dialyzed against the same buffer (150 mL) for 20 h to give SUVs with NBD-PE on both the inner and outer leaflet. In order to test the unilamellarity of the resulting vesicles, the vesicle suspension (9 μL, 0.5 μmol) was placed in a thermostated cuvette with gently stirred potassium phosphate buffer (2 mL), and then sodium dithionite (20 μL; 1 M in potassium phosphate buffer, pH adjusted to 6.4) was added. The fluorescence emission intensity of NBD (I_t; $\lambda_{ex} = 463$ nm, $\lambda_{em} = 536$ nm) was monitored during the operation (Figure 4c). After almost no change in fluorescence intensity was observed (~300 s), the detergent Triton X-100 (40 μL, 1.2%) was added to make all NBD groups accessible to dithionite in order to determine the endpoint. Compared to the fluorescence intensity before the addition of dithionite (I_0, 0% reduction) and after the addition of Triton X-100 (I_∞, 100% reduction), addition of dithionite to the vesicles caused 50% reduction of the fluorescence. This result indicated that only half the NBD groups in the vesicles were accessible to dithionite, therefore unilamellarity was assured.

Inner leaflet labeling: NBD-PE-doped EYPC-SUVs (290 μL, 16 μmol) were diluted with sodium phosphate buffer (1.6 mL, $Na_mH_nPO_4$ (10 mM), NaCl (100 mM), pH 6.4), and sodium dithionite (0.12 mL, 1 M) was added. After 15 min, the resulting vesicle suspension was passed through a Sephadex G-50 column (2 g) to separate remaining dithionite from the vesicles. The final concentration of lipid was adjusted to 4.5 mM. Inner-leaflet NBD-labeled EYPC-SUVs were used immediately after preparation.

Detection of flip-flop: Inner-leaflet NBD-labeled EYPC-SUVs (110 μL, 0.5 μmol) and potassium phosphate buffer (1.89 mL, $K_mH_nPO_4$ (10 mM), KCl (100 mM), pH 6.4) were placed in a thermostated cell. Changes in relative fluorescence intensity (I_t, $\lambda_{ex} = 463$ nm, $\lambda_{em} = 536$ nm) were recorded as a function of time during addition of $Mg(OAc)_2$ (0 or 10 mM final concentration) and barrel **1** (0 or 12.5 nM final concentration), incubation for around 100 s, and addition of sodium dithionite (20 mM) at time A [emission I at A corresponds to I_0 in Eq. (1)], and Triton X-100 (50 μL, 1.2% aq) at time B [emission I at B + 50 s corresponds to I_∞ in Eq. (1)] to the gently stirred vesicle suspension. Data were normalized with Eq. (1).

CD spectroscopy: CF-free EYPC-SUVs were prepared by dialytic detergent removal as previously described (diameter = 68 ± 4 nm).[2o, 5, 6, 11] Samples for UV/Vis (Varian Cary 1 Bio spectrophotometer) and CD spectroscopy measurements (JASCO-710 spectropolarimeter) were prepared by addition of EYPC-SUVs (10 mM EYPC, 25 μL), **1** (1.25 μM final concentration), $Mg(OAc)_2$ (final concentrations: 0 or 20 mM), and G-1-P or **2** (final concentrations: 0 – 80 mM) to stirred, thermostated buffer (1.00 mL; HEPES (10 mM), NaCl (107 mM), pH 6.5, 25 °C).

Measurements with G-1-P were made by using CD cells with a path length of 1.0 cm. $\Delta\varepsilon$ values refer to *p*-octiphenyl concentration. Dose response CD curves were prepared by using the $\Delta\varepsilon^{max}$ value at 305 nm.

Measurements with **2** were made by using CD cells with a path length of 0.1 cm. $\Delta\varepsilon$ values refer to polymer concentration and assume $N = 620$, for compatibility with pore blockage data. These values corresponded well with the $\Delta\varepsilon$ values of $0 - 2\,M^{-1}cm^{-1}$ previously calculated based on phosphonate concentration.[22a] Dose response CD curves were prepared by using the $\Delta\varepsilon^{max}$ value at 330 nm. Fractional saturation Y for CD Hill plots [Eq. (3)] were calculated by using Equation (4), where $\Delta\varepsilon_0^{330}$ is the $\Delta\varepsilon^{330}$ value without guest and $\Delta\varepsilon_\infty^{330}$ is the $\Delta\varepsilon^{330}$ value at saturation.

$$Y = \frac{(\Delta\varepsilon_0^{330} - \Delta\varepsilon^{330})}{(\Delta\varepsilon_0^{330} - \Delta\varepsilon_\infty^{330})} \quad (4)$$

We thank the Swiss National Science Foundation (Grant nos. 21 – 57059.99, 2000 – 064818.01 and National Research Program "Supramolecular Functional Materials" 4047 – 057496, S.M.) and Grant-In-Aid for Scientific Research from the Ministry of Education, Culture, Sports, Science and Technology of Japan (E.Y.) for financial support. We are also grateful to one reviewer for helpful suggestions.

[1] Reviews on synthetic ion channels and pores: a) G. W. Gokel, A. Mukhopadhyay, *Chem. Soc. Rev.* **2001**, *30*, 274; b) G. W. Gokel, *Chem. Eur. J.* **2001**, *7*, 33; c) D. T. Bong, T. D. Clark, J. R. Granja, M. R. Ghadiri, *Angew. Chem.* **2001**, *113*, 1016; *Angew. Chem. Int. Ed.* **2001**, *40*, 988; d) S. Matile, *Chem. Soc. Rev.* **2001**, *30*, 158; e) S. Matile, *Chem. Rec.* **2001**, *1*, 162; f) G. J. Kirkovits, C. D. Hall, *Adv. Supramol. Chem.* **2000**, *7*, 1; g) G. W. Gokel, *Chem. Commun.* **2000**, 1; h) R. N. Reusch, *Biochemistry (Moscow)* **2000**, *65*, 335; i) N. Sakai, S. Matile, *Chem. Eur. J.* **2000**, *6*, 1731; j) D. Seebach, M. G. Fritz, *Int. J. Biol. Macromol.* **1999**, *25*, 217; k) J. D. Hartgerink, T. D. Clark, M. R. Ghadiri, *Chem. Eur. J.* **1998**, *4*, 1367; l) Y. Kobuke, *Adv. Supramol. Chem.* **1997**, *4*, 163; m) U. Koert, *Chem. Unserer Zeit* **1997**, *31*, 20; n) G. W. Gokel, O. Murillo, *Acc. Chem. Res.* **1996**, *29*, 425; o) T. M. Fyles, W. F. van Straaten-Nijenhuis in *Comprehensive Supramolecular Chemistry* (Ed.: N. D. Reinhouldt) Elsevier, Oxford, **1996**, Vol. 10, p. 53; p) N. Voyer, *Top.*

Curr. Chem. **1996**, *184*, 1; q) R. J. M. Nolte, *Chem. Soc. Rev.* **1994**, 11; r) K. S. Åckerfeldt, J. D. Lear, Z. R. Wasserman, L. A. Chung, W. F. DeGrado, *Acc. Chem. Res.* **1993**, *26*, 191.

[2] Recent publications on synthetic ion channels and pores: a) L. M. Cameron, T. M. Fyles, C. Hu, *J. Org. Chem.* **2002**, *67*, 1548; b) P. H. Schlesinger, R. Ferdani, J. Liu, J. Pajewska, R. Pajewski, M. Saito, H. Shabany, G. W. Gokel, *J. Am. Chem. Soc.* **2002**, *124*, 1848; c) V. Sidorov, F. W. Kotch, G. Abdrakhmanova, R. Mizani, J. C. Fettinger, J. T. Davis, *J. Am. Chem. Soc.* **2002**, *124*, 2267; d) V. Janout, I. V. Staina, P. Bandyopadhyay, S. L. Regen, *J. Am. Chem. Soc.* **2001**, *123*, 9926; e) P. Bandyopadhyay, V. Janout, L.-H. Zhang, S. L. Regen, *J. Am. Chem. Soc.* **2001**, *123*, 7691; f) T. M. Fyles, R. Knoy, K. Müllen, M. Sieffert, *Langmuir* **2001**, *17*, 6669; g) T. M. Fyles, C. Hu, R. Knoy, *Org. Lett.* **2001**, *3*, 1335; h) A. J. Wright, S. E. Matthews, W. B. Fischer, P. D. Beer, *Chem. Eur. J.* **2001**, *7*, 3474; i) C. Goto, M. Yamamura, A. Satake, Y. Kobuke, *J. Am. Chem. Soc.* **2001**, *123*, 12152; j) N. Yoshino, A. Satake, Y. Kobuke, *Angew. Chem.* **2001**, *113*, 471; *Angew. Chem. Int. Ed.* **2001**, *40*, 457; k) H.-D. Arndt, A. Knoll, U. Koert, *ChemBioChem* **2001**, *2*, 221; l) H.-D. Arndt, A. Knoll, U. Koert, *Angew. Chem.* **2001**, *113*, 2137; *Angew. Chem. Int. Ed.* **2001**, *40*, 2076; m) J. Sanchez-Quesada, H. S. Kim, M. R. Ghadiri, *Angew. Chem.* **2001**, *113*, 2571; *Angew. Chem. Int. Ed.* **2001**, *40*, 2503; n) E. Biron, N. Voyer, J. C. Meillon, M.-E. Cormier, M. Auger, *Biopolymers* **2001**, *55*, 364; o) N. Sakai, D. Gerard, S. Matile, *J. Am. Chem. Soc.* **2001**, *123*, 2517; p) C. Pérez, C. G. Espínola, C. Foces-Foces, P. Núñez-Coello, H. Carrasco, J. D. Martín, *Org. Lett.* **2000**, *2*, 1185.

[3] Selected de novo α-helix bundle channels and pores: a) F. Nicol, S. Nir, F. C. Szoka, Jr., *Biophys. J.* **2000**, *78*, 818; b) T. C. B. Vogt, B. Bechinger, *J. Biol. Chem.* **1999**, *274*, 29115; c) G. R. Dieckmann, J. D. Lear, Q. Zhong, M. L. Klein, W. F. DeGrado, K. A. Sharp, *Biophys. J.* **1999**, *76*, 618; d) T. B. Wyman, F. Nicol, O. Zelphati, P. V. Scaria, C. Planck, F. C. Szoka, Jr., *Biochemistry* **1997**, *36*, 3008; e) J. D. Lear, J. P. Schneider, P. K. Kienker, W. F. DeGrado, *J. Am. Chem. Soc.* **1997**, *119*, 3212; f) L. H. Pinto, G. R. Dieckmann, C. S. Gandhi, C. G. Papworth, J. Braman, M. A. Shaughnessy, J. D. Lear, R. A. Lamb, W. F. DeGrado, *Proc. Natl. Acad. Sci. USA* **1997**, *94*, 11301; g) M. Dathe, T. Wieprecht, H. Nikolenko, L. Handel, W. L. Maloy, D. L. MacDonald, M. Beyermann, M. Bienert, *FEBS Lett.* **1997**, *403*, 208; h) S. Lee, T. Tanaka, K. Anzai, Y. Kirino, H. Aoyagi, G. Sugihara, *Biochim. Biophys. Acta* **1994**, *1191*, 181; i) R. A. Parente, S. Nir, F. C. Szoka, Jr., *Biochemistry* **1990**, *29*, 8720; j) N. K. Subbarao, R. A. Parente, F. C. Szoka, Jr., L. Nadasdi, K. Pongracz, *Biochemistry* **1987**, *26*, 2964; k) G. Menestrina, K.-P. Voges, G. Jung, G. Boheim, *J. Membr. Biol.* **1986**, *93*, 111.

[4] D. Wang, L. Guo, J. Zhang, L. R. Jones, Z. Chen, C. Pritchard, R. W. Roeske, *J. Pept. Res.* **2001**, *57*, 301.

[5] *p*-Octiphenyl β-barrel ion channels and pores: a) N. Sakai, S. Matile, *J. Am. Chem. Soc.* **2002**, *124*, 1184; b) B. Baumeister, S. Matile, *Macromolecules* **2002**, *35*, 1549; c) B. Baumeister, N. Sakai, S. Matile, *Org. Lett.* **2001**, *3*, 4229; d) G. Das, L. Ouali, M. Adrian, B. Baumeister, K. J. Wilkinson, S. Matile, *Angew. Chem.* **2001**, *113*, 4793; *Angew. Chem. Int. Ed.* **2001**, *40*, 4657; e) B. Baumeister, N. Sakai, S. Matile, *Angew. Chem.* **2000**, *112*, 2031; *Angew. Chem. Int. Ed.* **2000**, *39*, 1955; f) N. Sakai, B. Baumeister, S. Matile, *ChemBioChem* **2000**, *1*, 123; g) N. Sakai, N. Majumdar, S. Matile, *J. Am. Chem. Soc.* **1999**, *121*, 4294; h) N. Sakai, D. Houdebert, S. Matile, *Chem. Eur. J.*, submitted; i) B. Baumeister, A. Som, G. Das, N. Sakai, F. Vilbois, D. Gerard, S. P. Shahi, S. Matile, *Helv. Chim. Acta* **2002**, in press; j) A. Som, N. Sakai, S. Matile, unpublished results.

[6] G. Das, S. Matile, *Proc. Natl. Acad. Sci. USA* **2002**, *99*, 5183.

[7] a) L. C. Tarshis, P. J. Proteau, B. A. Kellogg, J. C. Sacchettini, C. D. Poulter, *Proc. Natl. Acad. Sci. USA* **1996**, *93*, 15018; b) C. A. Lesburg, G. Zhai, D. E. Cane, D. W. Christianson, *Science*. **1997**, *277*, 1820; c) C. R. Calladine, A. Sharff, B. Luisi, *J. Mol. Biol.* **2001**, *305*, 603.

[8] a) K. Matsuzaki, O. Murase, N. Fujii, K. Miyajima, *Biochemistry*, **1996**, *35*, 11361; b) U. Silphaduang, E. J. Noga, *Nature* **2001**, *414*, 268; c) L. Yang, T. A. Harroun, T. M. Weiss, L. Ding, H. W. Huang, *Biophys. J.* **2001**, *81*, 1475.

[9] For reviews on rigid-rod molecules, see, for example: a) M. D. Levin, P. Kaszynski, J. Michl, *Chem. Rev.* **2000**, *100*, 169; b) P. F. H. Schwab, M. D. Levin, J. Michl, *Chem. Rev.* **1999**, *99*, 1863; c) A. J. Berresheim, M. Müller, K. Müllen, *Chem. Rev.* **1999**, *99*, 1747; d) R. E. Martin, F. Diederich, *Angew. Chem.* **1999**, *111*, 1440; *Angew. Chem. Int. Ed.* **1999**, *38*, 1351.

[10] For some β barrels, see, for example: a) J. A. Gerlt, *Nat. Struct. Biol.* **2000**, *7*, 171; b) N. Nagano, E. G. Hutchinson, J. M. Thornton, *Protein Sci.* **1999**, *8*, 2072; c) S. K. Buchanan, *Curr. Opin. Struct. Biol.* **1999**, *9*, 445; d) G. Pujadas, J. Palau, *Biologia (Bratislava, Slovakia)* **1999**, *54*, 231; e) D. R. Flower, *Biochem. J.* **1996**, *318*, 1; f) M. H. Hecht, *Proc. Natl. Acad. Sci. USA* **1994**, *91*, 8729; g) J. S. Richardson, *Nature* **1977**, *268*, 495.

[11] a) L. A. Weiss, N. Sakai, B. Ghebremariam, C. Ni, S. Matile, *J. Am. Chem. Soc.* **1997**, *119*, 12142; b) C. Ni, S. Matile, *Chem. Commun.* **1998**, 755; and ref. [2o].

[12] a) M. M. Tedesco, B. Ghebremariam, N. Sakai, S. Matile, *Angew. Chem.* **1999**, *111*, 523; *Angew. Chem. Int. Ed.* **1999**, *38*, 540; b) B. Ghebremariam, V. Sidorov, S. Matile, *Tetrahedron Lett.* **1999**, *40*, 1445.

[13] a) G. Das, N. Sakai, S. Matile, *Chirality* **2002**, *14*, 18; b) G. Das, S. Matile, *Chirality* **2001**, *13*, 170; c) B. Baumeister, S. Matile, *Chem. Eur. J.* **2000**, *6*, 1739; d) B. Baumeister, S. Matile, *Chem. Commun.* **2000**, 913; for background on CD spectroscopy of higher arenes, see: e) K. Nakanishi, N. Berova, R. W. Woody, *Circular dichroism: principles and application*, VCH, Weinheim, **1994**; f) J. Sagiv, A. Yogev, Y. Mazur, *J. Am. Chem. Soc.* **1977**, *99*, 6861; g) B. Boreka, T. S. Cameron, A. Linden, P. Rashidi-Ranjbar, J. Sandström, *J. Am. Chem. Soc.* **1990**, *112*, 1185, and references cited therein.

[14] J.-H. Fuhrhop, J. Köning, *Membranes and Molecular Assemblies: The Cytokinetic Approach*, The Royal Society of Chemistry, Cambridge, UK, **1994**.

[15] R. P. Haugland, *Handbook of Fluorescent Probes and Research Chemicals,* 6th ed., Molecular Probes, Eugene OR, **1996**.

[16] Indicated concentrations refer to tetrameric supramolecule **1**; monomer concentrations are four times higher.

[17] a) K. A. Connors, *Binding Constants*, John Wiley & Sons, New York, **1987**; b) for K_D values of Mg^{2+} complexes (for example, aspartate: 4.0 mM, P_i: 3.2 mM, PP_i: 2.0 μM, PPP_i: 1.6 μM, ADP: 0.3 – 0.5 mM, ATP: 30 – 70 μM, DNA: 8.0 mM), see, for example, W. J. O'Sullivan, *Stability Constants of Metal Complexes*, in *Data for Biochemical Research,* 2nd ed. (Eds.: R. M. C. Dawson, D. C. Elliott, W. H. Elliot, K. M. Jones), Oxford University Press, Oxford, **1969**, pp. 423 – 434.

[18] For reviews on biological and synthetic poly- and oligo-*R*-3-hydroxybutyrate ion channels with internal, Ca^{2+}-complexed polyphosphates, see ref. [2h] and ref. [2j], respectively.

[19] a) D. Lim, S. Golovan, C. W. Forsberg, Z. Jia, *Nat. Struct. Biol.* **2000**, *7*, 108; b) S. R. Hull, J. S. S. Gray, R. Montgomery, *Anal. Biochem.* **1999**, *273*, 252, and references cited therein.

[20] a) S. Mathison, E. Bakker, *Anal. Chem.* **1999**, *71*, 4614; b) K. Gaus, E. A. Hall, *Biosens. Bioelectron.* **1998**, *13*, 1307; c) J. R. Fromm, R. E. Hileman, E. E. O. Caldwell, J. M. Weiler, R. J. Linhardt, *Arch. Biochem. Biophys.* **1995**, *323*, 279; d) R. Sasisekharan, G. Venkataraman, *Curr. Opin. Chem. Biol.* **2000**, *4*, 626.

[21] For binding and conversion of pyrene-1,3,6-sulfonates by histidine-rich *p*-octiphenyl β barrels with catalytic and ion-channel activity, see ref. [5c].

[22] a) H. Onouchi, K. Maeda, E. Yashima, *J. Am. Chem. Soc.* **2001**, *123*, 7441; b) K. Maeda, S. Okada, E. Yashima, Y. Okamoto, *J. Polym. Sci. Part A, Polym. Chem.* **2001**, *39*, 3180; c) E. Yashima, *Anal. Sci.* **2002**, *18*, 3; d) H. Kawamura, K. Maeda, Y. Okamoto, E. Yashima, *Chem. Lett.* **2001**, 58; e) K. Maeda, H. Goto, E. Yashima, *Macromolecules* **2001**, *34*, 1160; f) E. Yashima, K. Maeda, O. Sato, *J. Am. Chem. Soc.* **2001**, *123*, 8159.

[23] G. Das, S. Matile, unpublished results.

Received: April 19, 2002 [F402]